Multiscale-Multiphysics Modeling of Radiation-Damaged Materials: Embrittlement of Pressure-Vessel Steels

G.R. Odette, B.D. Wirth, D.J. Bacon, and N.M. Ghoniem

Introduction and Background

Radiation damage, and its attendant effect on a wide spectrum of materials properties, is a central issue in many advanced technologies ranging from ion-beam processing to the development of fusion power. Indeed, the various challenges presented by irradiation effects are too numerous to discuss in this brief article. However, the overarching fundamental objective of multiscale-multiphysics (MSMP) radiation effects modeling can be clearly stated: it is *predicting* the generation, transport, fate, and *consequences* of all defect species created by irradiation. Multiscale radiation-effects models are naturally hierarchical, establishing linkages upward from faster, more local processes and feedback downward from slower, larger-scale evolutions. The practical objective is to develop both improved materials performance and improved lifetime predictions based on relating property changes to the combination of a large number of material and irradiation variables. Models synthesize experimental information, ranging from laboratory-based mechanism studies to real-world surveillance data, and more reliably extrapolate beyond a limited and imperfect database.

Pertinent processes encompass the atomic nucleus ($\sim 10^{-15}$ m) all the way to structural-component length scales ($\sim$10 m), spanning more than 15 orders of magnitude. Time scales span more than 21 orders of magnitude, from the interaction time of neutron-atom collisions ($<10^{-15}$ s) to the 40–60-year operation lifetime of a nuclear reactor.

Radiation effects involve the interaction of a multitude of physical processes, which are briefly described in the next section. This emphasizes the importance of closely integrating models with experiment, including detailed microstructural characterization studies.

Although the range of materials, microstructures, physics, and properties that are encompassed by radiation effects is enormous, we focus on only one example—embrittlement of reactor pressure-vessel (RPV) steels. Further, due to the length restrictions of this article, only selected references are included; in many cases, they are representative of a much larger literature.

Embrittlement is a technologically and economically important problem, affecting the operation and safe lifetime of nuclear power plants around the world.[1] Severe embrittlement has led to both early plant closures and special annealing treatments for massive reactor vessels. A large research effort has been directed at developing improved methods for predicting embrittlement and resolving related problems. Much of the early work was purely empirical, but over the last decade, embrittlement has been a worldwide focus of fundamental research, including controlled experiments to identify the underlying mechanisms. Key parts of this research have involved the application and development of sophisticated tools for characterizing nanoscale embrittlement features, as well as modeling the causes and consequences of the nanostructural evolutions. Thus, the basic mechanisms of embrittlement are relatively well understood and most have been modeled.[2–31]

MSMP Processes in the Embrittlement of RPV Steels—A Modeling Architecture

A sequence of nuclear, atomic, solid-state, microstructure–property, and micromechanical processes combine to mediate radiation effects. The main objective of MSMP radiation-effects models is to link material and irradiation variables to microstructure evolution and, hence, to changes in key mechanical properties. In the case of the embrittlement of RPV steels at about 300°C and $<$0.1 displacements per atom, such evolution occurs at the nanoscale and involves formation of small defect-cluster–solute complexes and coherent (bcc) precipitates, usually enriched in copper. Copper, which is introduced as an impurity during processing and welding, is typically highly supersaturated prior to irradiation and quickly precipitates in alloys containing more than about 0.1% of this element, due to radiation-enhanced diffusion. Precipitates are enriched in nickel and manganese. Vacancies are currently believed to be the dominant defect in cluster complexes. These subnanometer clusters and nanoprecipitates lead to a significant increase in the yield strength, producing a corresponding elevation of the cleavage transition-temperature regime.[2–7]

Details of the various simulation and modeling methods are described elsewhere.[2–32] The availability and accuracy of interatomic potentials, including those for multiconstituent, multiphase alloys, is a major issue for MSMP modeling. In the results reported here, embedded-atom-type potentials are used for iron–iron and iron–copper interactions in molecular-dynamics and molecular-statics (MD and MS) simulations as well as kinetic lattice Monte Carlo (KLMC) simulations.[5,10–18,20,24] Lattice Monte Carlo (LMC) simulations of the composition of multi-element copper- and manganese-rich precipitates are based on even simpler, regular solution-type, pair-bonding potentials, derived from thermodynamic data in the literature.[4] The effect of potential uncertainties varies with the modeling task, but always needs careful consideration.

Figures 1, 2, and 3 illustrate the hierarchy of processes that must be integrated in a MSMP embrittlement model.

- Primary recoil atoms (PRAs): Neutron damage begins with the creation of energetic (typically a few tens of keV) PRAs from high-energy neutron–nuclear interactions. The cross sections and kinematics models needed to compute PRA spectra are incorporated in codes such as SPECTER.[9]
- Primary defect production in displacement cascades: The PRA kinetic energy is quickly transferred by a chain of subsequent atomic collision displacements, generating a cascade of vacancy and self-interstitial defects. This is simulated by MD codes that integrate the equations of motion of large assemblies of atoms (10^5–10^7), interacting by a known interatomic potential,[10–15] for times of the order of 100 ps, when most of the cascade thermal energy has dissipated (Figures 1a and 1b).[15] Many-body collisions lead to spatial separation of vacancies and self-interstitials and clustering of like defects. The large concentration of defects in high-energy PRA cascades results in substantial and rapid vacancy–interstitial recombination. Above approximately 1 keV, only about one-third of defects survive cascade vacancy–interstitial recombination. Libraries of results for MD cascade simulations[15–18] in iron have been used to derive primary defect production cross sections as a function of recoil energy,[13] not only for total vacancy–interstitial production, but also for the fractions and broad size classes of these defects located in cascade-generated clusters (Figure 1c).[14] While some residual questions remain, submodels of primary defect production for use in MSMP models are relatively well established.
- Cascade aging and delayed defect production: Spatial correlations continue to play an important role in longer-term evolution of the cascade defects. MD simulations show that most self-interstitial clusters are in the form of small prismatic $a/2\langle 111\rangle$ dislocation loops that are very mobile.[15–17] Mobile loops and isolated self-interstitials quickly leave the cascade region. Recombination during this phase has been treated by a KLMC simulation.[19]

The evolution of the remaining vacancy-rich cascade core has been modeled by KLMC.[20,21] Within milliseconds, most of the cascade vacancies jump short distances to form small, compact, three-dimensional clusters, while a small fraction leave the cascade region. The small clusters are unstable. However, they are also very mobile, and cluster diffusion–coalescence processes lead to the formation of larger, more stable nanovoids, containing tens of vacancies, prior to significant vacancy dissolution. In RPV alloys, solutes such as manganese,

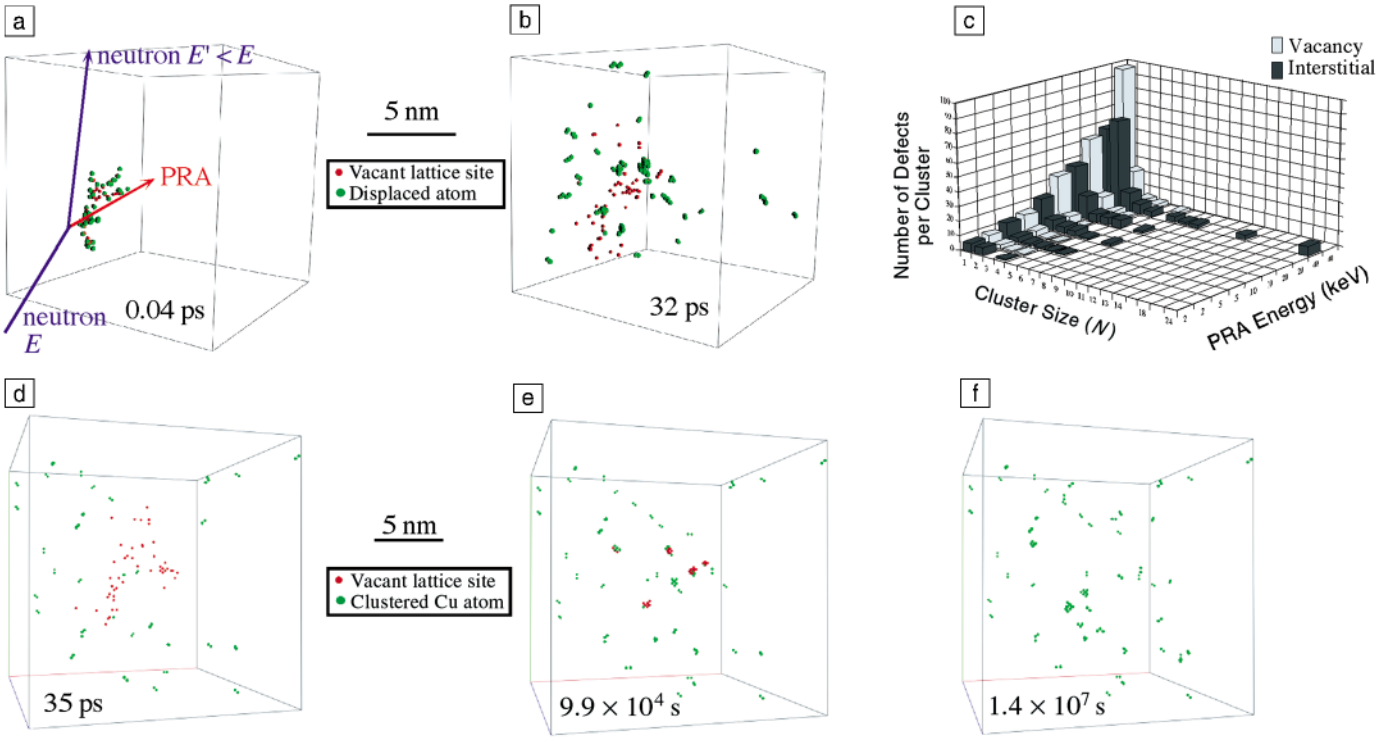

Figure 1. Defect production. (a), (b) A 20-keV molecular-dynamics cascade sequence showing a vacancy-rich core (red) and interstitial-rich shell (green).[15] (c) The nascent cascade cluster distribution (N is number of defects in a cluster) versus primary recoil atom (PRA) energy.[14] (d)–(f) Kinetic lattice Monte Carlo aging simulations of a 20-keV cascade in Fe-0.3%Cu.[20] E and E′ are the neutron energies before and after collision, respectively.

nickel, and copper bind to the vacancies, forming cluster complexes. KLMC simulations show that copper reduces vacancy emission rates from complexes with the same number of vacancies. Small vacancy–copper-cluster complexes also rapidly diffuse and coalesce, forming larger, less mobile complexes (Figures 1d and 1e)[20,21] that eventually dissolve, leaving behind small copper clusters (Figure 1f).[20] The larger cluster complexes persist up to more than 10^8 s. Over longer times, an excess vacancy flux and solute diffusion lead to additional growth of some cascade cluster complexes. Further modeling of cascade aging is a major area for future research.

■ Long-range defect migration: MD simulations show that self-interstitials and small clusters up to tetra-interstitials diffuse three-dimensionally, with intrinsic activation energies of only a few tenths of an electronvolt.[16–18] Larger interstitial cluster-dislocation $a/2\langle 111\rangle$ loops migrate by quasi one-dimensional diffusion along their glide prism, with activation energies of <0.1 eV (Figure 2a).[16–18] Sink interactions, solute trapping, and reorientation probability of the glissile loops are directly amenable to MD modeling. For example, very recent MD results[22] suggest a minimal effect of 1.0% oversized copper on the migration of a small ten-interstitial cluster.

Excess defects lead to radiation-enhanced (solute) diffusion. KLMC methods have been used to simulate diffusion coefficients by vacancy exchange in iron-copper alloys (Figure 2b).[20] The corresponding radiation-enhanced copper diffusion coefficient (Figure 2c)[3] is determined by rate-theory (RT) models of vacancy concentration that treat the effect of temperature, defect-generation rate, sink strength, solute and cascade cluster concentration, and solute–vacancy binding energies. Trapping, annihilation, and absorption of mobile defects at copper precipitates must be included in future models. Another very recent MD–MS study has shown that energy increases as a glissile loop approaches a coherent copper precipitate with a positive mismatch strain (Figure 2d).[22] MD studies of interstitial cluster interactions must be extended to other defects and microstructural features.

■ Nanostructural and nanochemical evolutions: The solubility limit of copper is <0.01% at around 300°C. A high number ($\geq 10^{23}$ m^{-3}) of small (~1.5–3-nm diameter), coherent (bcc), copper-rich precipitates (CRPs) are the dominant feature in steels with more than ~0.1% copper.[2,3] Copper precipitation is rapid due to radiation-enhanced diffusion. Precipitate evolution under irradiation and post-irradiation annealing has been treated using multistate kinetics RT models.[3,7,23] Large sets of differential equations, with terms for the formation and loss rates of discrete cluster classes of i copper atoms are integrated to predict cluster evolution by nucleation, growth, and coarsening (Figure 2e).[3] Transition-rate coefficients are based on typical RT approximations with boundary conditions set by alloy matrix and local-equilibrium precipitate–complex thermodynamics. Solutes flow down gradients based on the difference in their activity in the matrix and precipitate, including the effect of the composition-dependent interface energy. This results in enrichment of manganese and nickel (and other elements) in CRPs, and formation of

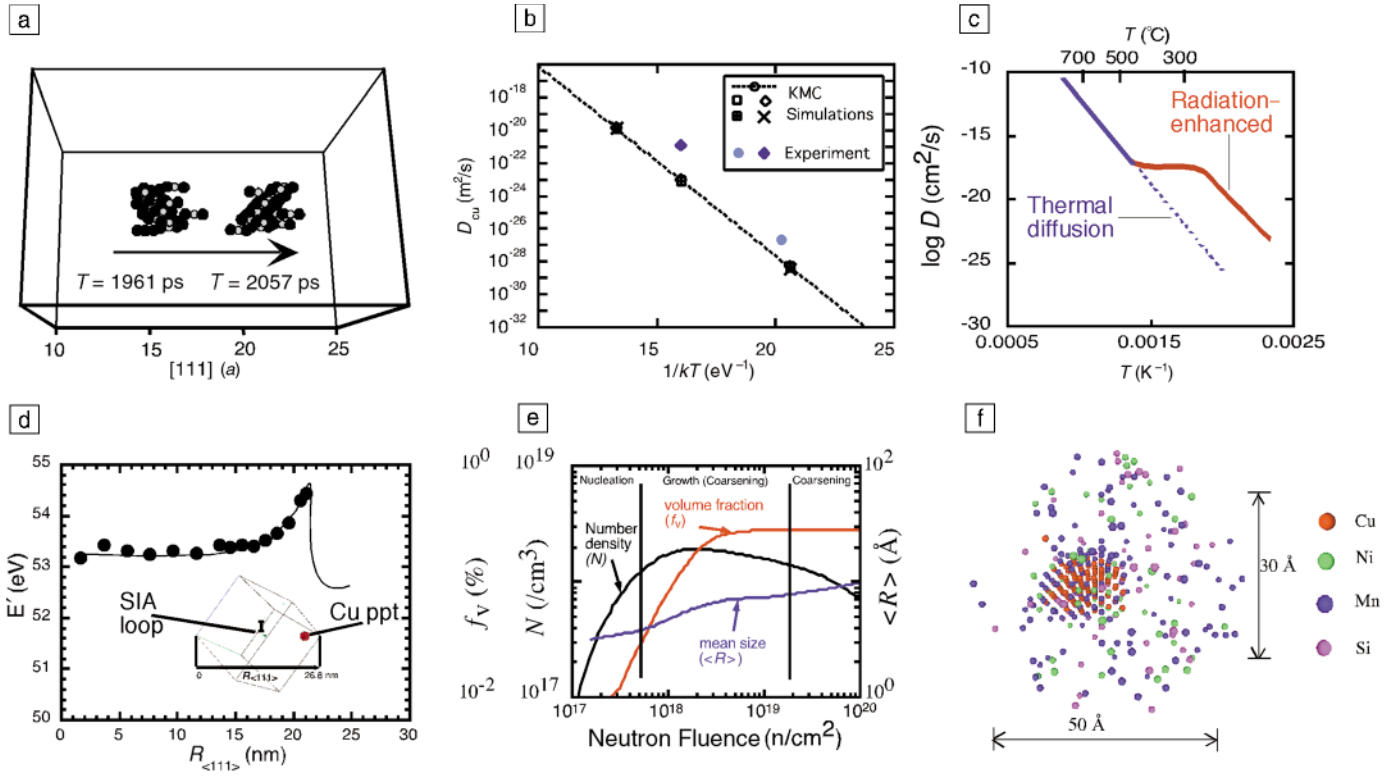

Figure 2. Long-range migration and clustering of defects and solutes. (a) Initial and final position of a small self-interstitial cluster.[18] (b) Kinetic Monte Carlo simulations of copper diffusion.[20] (c) Rate-theory model predictions of the radiation-enhanced diffusion of copper.[3] (d) Molecular-statics simulations of the potential-energy increase as an interstitial loop approaches a copper-rich precipitate (CRP). (e) A multistate kinetics rate-theory model of the nucleation, growth, and coarsening of CRPs at 290°C in an Fe-0.4%Cu alloy.[3] (f) A lattice Monte Carlo simulation of the composition and structure of a CRP in an Fe-0.24%Cu-0.59%Ni-1.50%Mn-1.0%Si alloy at 290°C.[4]

manganese–nickel-rich precipitates (MNPs) in some alloy composition–temperature regimes. The models assume that the radiation-enhanced diffusion of copper is rate-controlling. The fluxes of other elements are assumed to be proportional to the copper flux, based on the ratios predicted by a thermodynamic assessment of solute flows to a relatively small number of precipitate size classes.

LMC has also been used to directly simulate the composition and structure of CRPs and MNPs.[4] The results are broadly consistent with the mean-field thermodynamics model predictions, but provide atomic-level detail on these features. The polyhedral, coherent precipitates typically have a copper-rich core surrounded by, and sometimes appended to, manganese–nickel-rich regions (Figure 2f).[4] The manganese–nickel-rich regions tend to be ordered. Such information is important for interpreting the results of high-resolution nanostructural characterization studies.[3,4]

Some of the defect-cluster–solute complexes generated in cascades grow due to long-range solute diffusion and a biased flux of vacancies. To date, multistate kinetics RT models have been used to treat only vacancy-cluster evolution, using adjustments to the surface energy to crudely account for some complex composition effects.[7] More general RT treatments of cluster-complex evolution of the simultaneous clustering of excess vacancies and solutes are being developed.

In summary, both rate-theory and lattice Monte Carlo models of CRP (and MNP) evolution under irradiation and annealing are broadly consistent with experiment and can be incorporated in MSMP models. Extension of the multi-element LMC precipitate models to KLMC simulations that include vacancies, and ultimately interstitials, is a target of future research. This extension is particularly important in modeling longer-term evolutions of the vacancy-cluster–solute complexes, initially formed in aged cascades.

■ Irradiation-induced increases in the yield stress: Nanoscale features produce substantial increases in the yield stress ($\Delta\sigma_y$) by acting as dispersed obstacles to dislocation slip. Modeling $\Delta\sigma_y$ requires treating both (a) the obstacle strengths (β) and the strength contribution (σ_i) of the individual features, and (b) the collective effect of these relatively weak features in combination with preexisting strong obstacles that are unaffected by irradiation. The strength factor β, which varies with the type and size of the obstacle, is a measure of maximum force needed for the dislocation to cut through a weak obstacle or bow around a strong obstacle.[24] Recently, MD simulations have been used to study the interaction of dislocations with various defect and solute aggregations.[25] The effective pinning force is given by the maximum in the derivative of the energy versus dislocation position curve (similar unpublished results have been obtained by S. Jumel et al.[26]). For example, the interaction of a screw dislocation with a coherent copper precipitate leads to a transformation of the metastable bcc to a fcc-like structure[25] that makes the major contribution to the energy reduction (Fig-

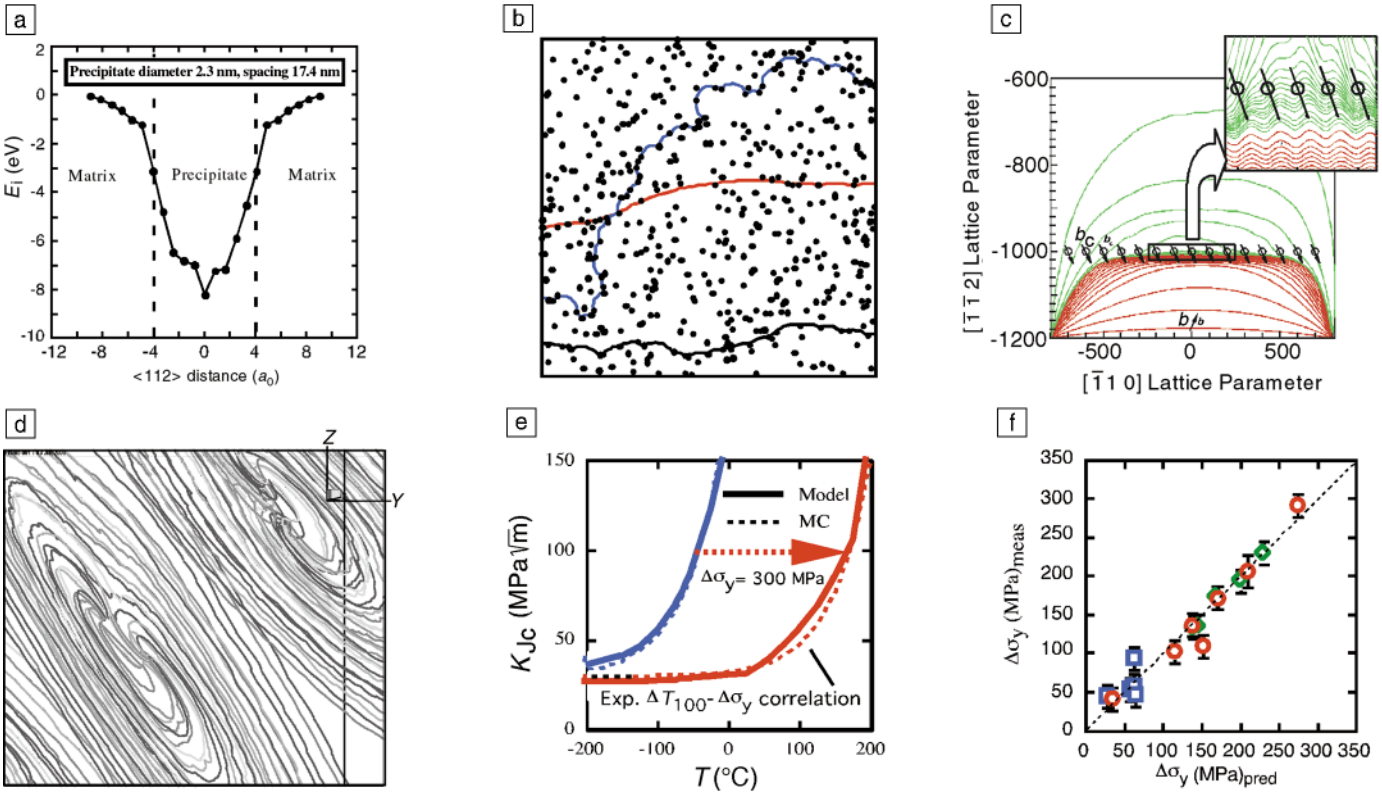

Figure 3. Changes in constitutive and fracture properties due to nanostructural evolutions. (a) Molecular-dynamics simulation of the energy of a screw dislocation interacting with a copper precipitate.[24] (b) Simulation of dislocations interacting with weak (red), intermediate (black), and strong (blue) obstacles at yield.[6] (c) Dislocation-dynamics simulation of dislocation configurations bypassing an atmosphere of defect clusters;[25] b_c refers to the Burgers vector of the defect clusters. (d) Dislocation-dynamics simulation of the generation of deformation channels in copper from dislocation interactions with stacking-fault tetrahedra.[26] (e) Micromechanical model predictions of fracture toughness compared with an invariant master-curve (MC) shape, including the effect of a 300-MPa increase in yield stress.[29] (f) Predictions of CRP hardening, compared with experiment.[6,20]

ure 3a),[25] hence, the pinning strength. The corresponding prediction of β is consistent with experiment.

The second issue in modeling $\Delta\sigma_y$ is how σ_i combines with, or is superimposed on, the contribution to the unirradiated obstacle strength (σ_u) from preexisting larger and stronger obstacles such as Mo_2C particles, which are bypassed by the Orowan bowing mechanism. This problem was originally studied by Foreman and Makin[24] for two obstacle strengths. More recent computer simulations of the stresses needed to move a single dislocation through an array of weak ($\beta_w < 0.4$) and strong ($\beta_s > 0.6$) obstacle configurations with a range of strengths (Figure 3b)[6] showed that the superposition can be described by a parameter S that weights the balance between linear and root sum superposition limits: $\Delta\sigma_y = S\,[(\sigma_i^2 + \sigma_u^2)^{1/2}] - \sigma_u + (1 - S)\sigma_i$. Further, S depends primarily on β_s, and on β_w in a way that can be described by a simple analytical expression.[6]

- Dislocation dynamics (DD): The $\Delta\sigma_y$ models described in the previous section are based on a number of assumptions and approximations and do not treat the critical issues of post-yield and localized deformation. All of these problems can be addressed with dislocation dynamics.[27,28] For additional information, see the article by Bulatov, Tang, and Zbib in this issue. The DD approach directly simulates three-dimensional interactions of large numbers of discretized (in curved or straight segments) dislocations for general conditions of source configurations, obstacle types and distributions, and boundary conditions. Very efficient and mathematically elegant computational algorithms have been developed to permit self-consistent treatments of elastic interactions of all of the segments. The method also incorporates physically based submodels of important local processes such as nucleation of kinks and cross slip, dislocation reactions, obstacle interaction mechanisms, energetics and reaction paths, and dislocation velocity-stress relations. Thus, DD can simulate strain hardening in pure crystals as well as many other phenomena such as source and dispersed obstacle hardening[29] pertinent to irradiation effects. The submodels provide a direct link to both atomistic simulations and dislocation theory.

So far, DD simulations have not been used for modeling embrittlement. However, given the importance of DD to future progress, a few examples are briefly noted. DD has been used to simulate source hardening in copper due to an atmosphere of sessile dislocation loops, at a stand-off distance prescribed by trapping energetics. The DD simulations reveal that the interplay between the stand-off distance, cluster spacing, and the evolution of an asymmetric dislocation shape leads to an instability at a critical stress that unlocks the source (Figure 3c)[27] due to the dislocation shape flexibility that cannot be captured in analytical treatments. The second example involves the seminal problem of flow localization, associated with the annihilation of defect-cluster obstacles by slip dislocations.[28] One plausible mechanism in copper is that dislocation interactions re-dissolve and absorb the vacancies in stacking-fault tetrahedra, resulting in climb of a dislocation segment, terminating at adjoining sessile jogs, and continuing slip on another plane. Operation of preexisting sources and propagation of self-generated climb sources lead to channel thickness and spacing dimensions that are consistent with experiment (Figure 3d).[28]

- Shifts in fracture toughness versus temperature master curves: Changes in the constitutive properties result in degradation of the fracture resistance of RPV steels manifested as shifts (ΔT) in the cleavage transition temperature.[7,3,30] Micromechanical models have been developed to relate $\Delta\sigma_y$ to the temperature shifts at 41 J for standard Charpy tests.[7,30] However, the effect of irradiation on the K_{Jc} temperature-dependence of fracture toughness [$K_{Jc}(T)$] is of far greater interest. Furthermore, recent empirical observations suggest that the $K_{Jc}(T)$ may have a universal master-curve shape.[31] This behavior has been rationalized by preliminary results of a MSMP cleavage model that predicts both approximate shape invariance and the corresponding ΔT caused by irradiation-induced $\Delta\sigma_y$ *and* related changes in strain hardening[32] (Figure 3e). The model is based on the concept that cleavage occurs when a critical stress (σ^*) contour in front of a blunting crack envelops a critical region containing brittle cleavage trigger particles, such as large grain-boundary carbides. Finite element analysis, with appropriate constitutive properties, is used to compute the crack-tip stress–strain fields. It has been generally assumed that σ^* depends on the size of the trigger particles but is independent of both temperature and irradiation. The key insight in the new model is that σ^* is actually a weak function of temperature in the regime where the Peierls stress is small.[32] The σ^* is controlled by the intrinsic ferrite toughness, which is in turn controlled by the emission of dislocations and the development of dislocation structures at the tip of the nanoblunting microcrack, which emanate from a broken brittle trigger particle. Detailed DD and MD modeling of dynamic nanoblunting-cleavage decohesion is an important next step in MSMP of cleavage $K_{Jc}(T)$ curves.

Progress on a Fully Integrated MSMP Hardening and Embrittlement Model

While they are certainly neither perfect nor fully based on first principles, physical submodels are now available for all of the key MSMP processes mediating irradiation-embrittlement of RPV steels. Indeed, models have often led experimental observations of key embrittlement phenomena.[2,3] Small-angle neutron-scattering measurements of CRPs have been used

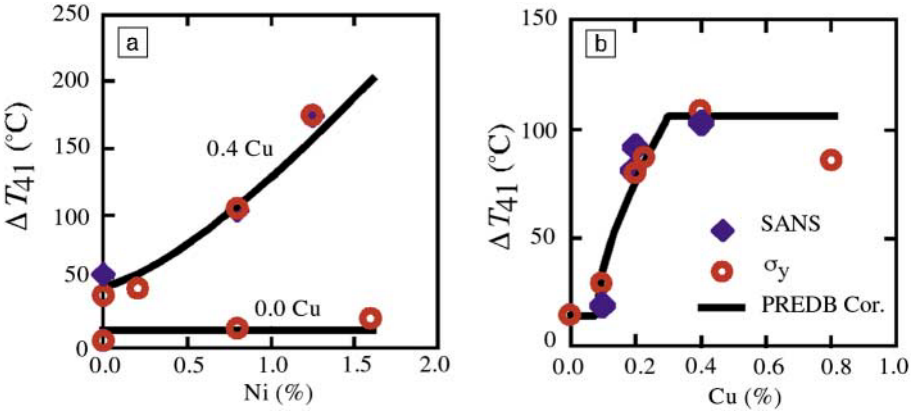

Figure 4. An integrated embrittlement model. Predicted irradiation-induced Charpy transition-temperature shifts (T_{41}, measured at an energy of 41 J) as a function of (a) nickel and (b) copper. These results are based on combining a hardening-shift model with yield-stress increases derived either directly from tensile tests or from using small-angle neutron-scattering characterization of the CRPs in the hardening model. The solid lines are the corresponding predictions based on a totally independent power-reactor engineering database correlation (PREDB Cor.) of Charpy data.[8]

to successfully predict $\Delta\sigma_y$, based on the hardening models described earlier (Figure 3f).[6,20] Corresponding predictions of the effects of copper and nickel (and other variables) on Charpy shifts are remarkably consistent with completely independent statistical fits to a large (607 data points) power-reactor engineering database (Figures 4a and 4b).[8] More generally, existing models rationalize almost all observed embrittlement trends, including those that are counterintuitive and complex, such as seemingly contradictory effects of neutron flux.[6,7]

The development of detailed simulations of cluster complex evolution and the full integration of all key submodels into a unified and quantitatively predictive MSMP embrittlement model is now under way in a collaboration between the University of California—Santa Barbara, Oak Ridge National Laboratory, and Lawrence Livermore National Laboratory. There is also a similar activity in Europe. Both activities are being coordinated through the international REVE project led by Prof. Jean-Claude Van-Duysen. Implementation of a fully integrated, albeit still simplified and approximate, MSMP model will have some substantial advantages. These include a direct and rigorous accounting of defect and solute redistribution balances, better treatment of highly coupled processes such as vacancy trapping and radiation-enhanced diffusion of solutes, and the inclusion of the effects of evolving sinks and trapping structures. Furthermore, an integrated model will provide a framework for testing the impact of alternative and improved submodels. Finally, an integrated model will provide a convenient tool for interpreting and analyzing data ranging from nanoscale characterization studies to quantitative statistical fits to engineering data.

Closing Remarks

This article reviewed the recent efforts to develop key component parts and simulation tools for the near-term assembly of a fully integrated multiscale-multiphysics (MSMP) model of irradiation embrittlement of RPV steels. Additional research needed to refine many of these parts and to develop more advanced tools was also briefly outlined. Initially, any integrated model will certainly not be perfect, as must be expected when confronting a problem of such complexity. Nevertheless, an integrated MSMP model will manifest many advantages over more empirical and ad hoc approaches, not the least of which is providing a convenient framework for continued, systematic improvements. In a more general sense, progress in MSMP modeling of embrittlement provides a clear example for other applications in radiation effects, as well as other areas of materials science. Steady progress will entail building a knowledge base that is far more accessible and useful (e.g., for design of new materials) than traditional approaches.

Acknowledgments

Support for substantial portions of this work was provided by the U.S. Nuclear Regulatory Commission and the U.S. Department of Energy.

References

1. *Radiation Embrittlement of Reactor Vessel Materials,* Regulatory Guide 1.99, Rev. 2 (U.S. Nuclear Regulatory Commission, Washington, DC, May 1988).
2. G.R. Odette, *Scripta Metall.* **11** (1983) p. 1183.
3. G.R. Odette, in *Microstructure of Irradiated Materials,* edited by I.M. Robertson, L.E. Rehn, S.J. Zinkle, and W.J. Phythian (Mater. Res. Soc. Symp. Proc. **373**, Pittsburgh, 1995) p. 137.
4. G.R. Odette, C.L. Liu, and B.D. Wirth, in *Microstructure Evolution During Irradiation,* edited by I.M. Robertson, G.S. Was, L.W. Hobbs, and T. Diaz de la Rubia (Mater. Res. Soc. Symp. Proc. **439**, Pittsburgh, 1997) p. 457.
5. G.R. Odette and B.D. Wirth, *J. Nucl. Mater.* **251** (1997) p. 157.
6. G.R. Odette and G.E. Lucas, *Radiat. Eff. Defects Solids* **144** (1998) p. 189.
7. G.R. Odette, in *Neutron Irradiation Effects in Reactor Pressure Vessel Steels and Weldments,* IAEA IWG-LMNPP-98/3, edited by M. Davies (International Atomic Energy Agency, Vienna, 1998) p. 438.
8. E.D. Eason, J.E. Wright, and G.R. Odette, *Improved Embrittlement Correlations for Reactor Pressure Vessel Steels,* NUREG/CR-6551 (U.S. Nuclear Regulatory Commission, Washington, DC, 2000).
9. L.R. Greenwood and R.K. Smither, technical report, ANL/FPP-TM-197 (Argonne National Laboratory, Argonne, IL, 1985).
10. A.F. Calder and D.J. Bacon, *J. Nucl. Mater.* **207** (1993) p. 25.
11. R.E. Stoller, G.R. Odette, and B.D. Wirth, *J. Nucl. Mater.* **251** (1997) p. 49.
12. R.S. Averback and T. Diaz de la Rubia, *Solid State Phys.* **51** (1998) p. 281.
13. R.E. Stoller, *Nucl. Eng. Des.* **195** (2000) p. 129.
14. D.J. Bacon, F. Gao, and Y.N. Osetsky, *J. Comput.-Aided Mater. Des.* **6** (1999) p. 225.
15. R.E. Stoller, in *Microstructure of Irradiated Materials,* edited by I.M. Robertson, L.E. Rehn, S.J. Zinkle, and W.J. Phythian (Mater. Res. Soc. Symp. Proc. **373**, Pittsburgh, 1995) p. 21.
16. N. Soneda and T. Diaz de la Rubia, *Philos. Mag. A* **78** (1998) p. 995.
17. B.D. Wirth, G.R. Odette, D. Maroudas, and G.E. Lucas, *J. Nucl. Mater.* **276** (2000) p. 33.
18. Y.N. Osetsky, D.J. Bacon, A. Serra, B.N. Singh, and S.I.Y. Golubov, *J. Nucl. Mater.* **276** (2000) p. 65.
19. M.J. Caturla, N. Soneda, E.A. Alonso, B.D. Wirth, and T. Diaz de la Rubia, *J. Nucl. Mater.* **276** (2000) p. 13.
20. B.D. Wirth, "On the Character of Nanoscale Features in Reactor Pressure Vessel Steels Under Neutron Irradiation," PhD dissertation, University of California—Santa Barbara, 1998.
21. B.D. Wirth and G.R. Odette, in *Microstructural Processes in Irradiated Materials,* edited by S.J. Zinkle, G.E. Lucas, R.C. Ewing, and J.S. Williams (Mater. Res. Soc. Symp. Proc. **540**, Warrendale, PA, 1999) p. 637.
22. J. Marian, B.D. Wirth, J.M. Perlado, G.R. Odette, and T. Diaz de la Rubia, in *Microstructural Processes in Irradiated Materials,* edited by G.E. Lucas, L.L. Snead, M.A. Kirk, and R.G. Elliman, (Mater. Res. Soc. Symp. Proc. **650**, Warrendale, PA, 2001) in press.
23. E.V. Mader, "Kinetics of Irradiation Embrittlement and the Post-Irradiation Annealing of Nuclear Reactor Pressure Vessel Steels," PhD dissertation, University of California—Santa Barbara, 1995.
24. A.J.E. Foreman and M.J. Makin, *Can. J. Phys.* 45 (1967) p. 511.
25. T. Harry and D.J. Bacon, in *Microstructure Evolution During Irradiation,* edited by I.M. Robertson, G.S. Was, L.W. Hobbs, and T. Diaz de la Rubia (Mater. Res. Soc. Symp. Proc. **439**, Pittsburgh, 1997) p. 495.
26. S. Jumel and J.C. Van-Duysen (private communication, 2000).
27. N.M. Ghoniem and L.Z. Sun, *Phys. Rev. B* **60** (1999) p. 128.
28. N.M. Ghoniem, S.-S. Tong, and L.Z. Sun, *Phys. Rev. B* **61** (2) (2000) p. 913.
29. J. Friedel, *Dislocations* (Pergamon Press, Oxford, 1964).
30. G.R. Odette, P.M. Lombrozo, and R.A. Wullaert, in *Effects of Radiation on Materials: 12th International Symposium,* ASTM-STP-870, edited by F.A. Garner and R.S. Perrin (American Society for Testing and Materials, Philadelphia, 1985) p. 841.
31. K. Wallin, *Int. J. Mater. Prodt. Technol.* **14** (1999) p. 342.
32. G.R. Odette and M.Y. He, *J. Nucl. Mater.* **283–287** (2000) p. 120. □